Supplement of

Measurement report: Distinct urban and rural organonitrate formation regimes in a mixed anthropogenic-biogenic subtropical atmosphere

Shan Huang et al.,

Correspondence to: Shan Huang (shanhuang_eci@jnu.edu.cn)

Text S1 PMF solution and ON derived from PMF-method

S1.1 PMF_{OA+NOx} at the urban and rural site (Laser off mode)

Based on the PMF results of organic aerosol (PMF_{org}), NO^+ and NO_2^+ fragments were added to the high-resolution organic mass spectral matrix (HROrg), and the PMF model was recalculated with factor number from 1 to 10. A 7-factor solution was selected for both urban and rural sites, with diagnostic plots shown in Figs. S2 and S3. The optimal number of factor was determined by the change in Q/Q_{exp} with increasing factors, following the criterion of a substantial decrease in Q/Q_{exp} (as a turning point). At both urban and rural sites, a 6-factor solution failed to separate the primary factors (HOA and COA at the urban site, and HOA and BBOA at the rural site), while an 8-factor solution produced no additional interpretable factors. Accordingly, combined with PMF_{org} results, a 7-factor solution was determined as the optimal representation of $PMF_{Org+NOx}$ at both sites. After the factor number was fixed, rotational forcing parameter (fPeak) was varied from −1 to 1 in steps of 0.2 to examine solution stability and uniqueness. For the 7-factor solution, the factor contributions remained relatively stable across different fPeak values, confirming the robustness and interpretability of the chosen solution. Finally, fPeak = 0 and fPeak = −0.2 were selected for the urban and rural sites, respectively. For the rural site, the fPeak = −0.2 solution was preferred because it gave the best correlations with the PMF_{org} factors in both mass spectra and time series.

Details of the selected 7-factor solutions for both sites, including mass spectra, time series, and diurnal variations, are displayed in Figs. S4 and S5, respectively. Similar with PMF_{org}, six organic factors and one inorganic nitrate factor (Inorg-NO_3) were identified. The organic factors from $PMF_{Org+NOx}$ are well correlated with the corresponding PMF_{Org} factors (Table S2), with mass spectral correlations (R) of 0.70–0.98 and time-series correlations (R) of 0.87–0.99, confirming that they represent the same sources. The NO_3^+ signal (sum of NO^+ and NO_2^+) extracted from each organic factor is interpreted as the organic nitrate contributed by that source.

S1.2 $PMF_{OA+Cx+NOx}$ at the urban and rural site (Laser on mode)

Because the SP-AMS in dual-vaporizer (laser-on) mode simultaneously provides the chemical composition of both non-refractory and refractory (primarily BC and BC coatings) aerosol components, we extended the PMF analysis by adding the C_x^+(C_1^+~C_9^+) and NO_x fragments from SP mode to the HR organic mass spectral matrix,

i.e., $PMF_{Org+Cx+NOx}$. The corresponding PMF diagnostic plots for the urban and rural sites are shown in Figs. S6 and S7, respectively. As with the laser-off mode ($PMF_{Org+NOx}$), a 7-factor solution was selected as the optimal one, resolving six organic factors and one inorganic nitrate factor (Inorg-NO_3). The detailed results of the selected 7-factor solution for the urban and rural sites in laser-on mode, including mass spectra, time series, and diurnal variations, are displayed in Figs. S8 and S9, respectively.

Good agreement was also found between the factors derived from the laser-on and laser-off modes at both sites (Table S3), with mass spectral correlations (R) of 0.73–0.99 and time-series correlations (R) of 0.64–0.94. All organic factor concentrations were higher in laser-on mode than in laser-off mode, as indicated by the slopes of the time-series regressions for the OA factors, which ranged from 1.16 to 1.34 at the urban site and from 1.24 to 1.91 at the rural site. The NO3+ signal (sum of NO^+ and NO_2^+) extracted from each organic factor in $PMF_{Org+Cx+NOx}$ is interpreted as the organic nitrate contributed by that source, inclusive of the refractory fraction.

Text S2 NOx ratio method of ON

The NO_X ratio method distinguishes organic nitrates (ON) from inorganic nitrate using their distinct NO^+/NO_2^+ ratio (R_{ON} and R_{AN})(Boyd et al., 2015; Bruns et al., 2010; Farmer et al., 2010; Fry et al., 2009). ON-derived NO^+ and NO_2^+ can be estimated via Eqs. (1) and (2):

$$NO_{2,ON}^{+} = \frac{NO_{2,meas}^{+} \times (R_{meas} - R_{AN})}{R_{ON} - R_{AN}} \quad (1)$$

$$NO_{ON}^{+} = R_{ON} \times NO_{2,ON}^{+} \quad (2)$$

where R_{meas} is the measured ratio. R_{AN} was set to 1.10 (ammonium nitrate calibrations) for the urban site and 2.0 (Inorg-NO_3 factor) for the rural site. Given that R_{ON}/R_{AN} is independent of the instrument (Boyd et al., 2015), 2.08 and 3.99 for RON/RAN ratios (Farmer et al., 2010; Boyd et al., 2015; Bruns et al., 2010; Sato et al., 2010; Xu et al., 2015a) were used as the upper and lower boundary for ON estimation. Although Day et al. (2022) converted the equations and validated the approach using an average ratio (RAN/RON = 2.75), both that work and our own experience (Liao et al., 2026) indicate that the method can yield a few points of organonitrate fractions exceeding total nitrate ($NO_{3,org}/NO_3 > 1$). Accordingly, upper- and lower-bound organonitrate values are reported here for method intercomparison.

Table S1 Instrumentation at both sites.

Instrument	Abbreviation	Manufacturer / Model	Original Time Resolution	Deployed site
Soot Particle High-Resolution Time-of-Flight Aerosol Mass Spectrometer	SP-HR-ToF-AMS (SP-AMS)	Aerodyne Research, Inc. MA, USA	1 min (raw); averaged to 10 min (urban) / 15 min (rural)	Both
Scanning Mobility Particle Sizer	SMPS	TSI Inc. model 3082	4min	Both
Online Gas Chromatography-Mass Spectrometry / Flame Ionization Detector	GC-MS/FID	Wuhan Tianhong Co., Ltd, China	1h	Both
High-Resolution Proton Transfer Reaction Time-of-Flight Mass Spectrometry	PTR-ToF-MS	Ionicon Analytik, Austria	1min	Both
Ozone Analyzer	O3 Analyzer	Thermo Fisher Scientific Inc. model 49i	1h	Both
NOx Analyzer	NOx Analyzer	Thermo Fisher Scientific Inc. model 42i	1h	Both
Carbon Monoxide Analyzer	CO Analyzer	Thermo Fisher Scientific Inc. model 48i	1h	Both
Meteorological Sensors	–	Supplied by local environmental authority	1h	Both
Filter Inlet for Gases and AEROsols – Chemical Ionization Mass Spectrometer	FIGAERO-CIMS	Aerodyne Research, Inc. MA, USA	1 h	Both

Table S2 Correlation coefficients (R) and slopes of linear regression between factors from PMF_{org} and $PMF_{org+NOx.}$(Laser off)

PMF factors		**HOA**		**COA**		**LOOA**		**MOOA**		**aBBOA**		**NOA**	
Org **vs**. Org+NO_x^+		MS	TS	MS	TS	MS	TS	MS	TS	MS	TS	MS	TS
Urban	slope	0.83	1.54	0.64	0.63	0.95	0.93	0.94	0.85	0.78	1.01	0.84	1.02
	R	0.86	0.92	0.80	0.96	0.95	0.98	0.96	0.95	0.91	0.95	0.70	0.99
PMF factors		**HOA**		**BBOA**		**LOOA**		**MOOA**		**BBSOA**		**Night-OA**	
Org **vs.** Org+NO_x^+		MS	TS	MS	TS	MS	TS	MS	TS	MS	TS	MS	TS
Rural	slope	0.56	0.96	0.88	0.91	0.95	0.96	0.98	0.93	0.81	0.93	0.76	0.87
	R	0.74	0.99	0.91	0.99	0.86	0.99	0.98	0.98	0.78	0.98	0.75	0.87

Table S3 Correlation coefficients (R) and slopes of linear regression between factors from $PMF_{org+NOx}$ (laser off) and $PMF_{org+Cx+NOx}$ (laser on).

PMF factors		**HOA**		**COA**		**LOOA**		**MOOA**		**aBBOA**		**NOA**	
$Org+NO_x^+$ **vs.** $Org+NO_x^++C_x$		MS	TS	MS	TS	MS	TS	MS	TS	MS	TS	MS	TS
Urban	slope	0.89	1.25	0.98	1.16	0.97	1.32	1.01	1.28	0.99	1.34	0.95	1.28
	R	0.99	0.94	0.99	0.96	0.99	0.97	0.99	0.78	0.99	0.64	0.99	0.93
PMF factors		**HOA**		**BBOA**		**LOOA**		**MOOA**		**BBSOA**		**Night-OA**	
$Org+NO_x^+$ **vs.** $Org+NO_x^++C_x$		MS	TS	MS	TS	MS	TS	MS	TS	MS	TS	MS	TS
Rural	slope	0.91	1.24	0.91	1.74	0.91	1.66	0.84	1.91	0.91	1.34	1.39	1.29
	R	0.99	0.67	0.97	0.73	0.99	0.95	0.98	0.81	0.99	0.75	0.73	0.74

Table S4 Rate coefficients and branching ratio used for the calculation of PP_{ON}

Num	VOC	k(OH) at 298K (molecules cm^{-3} s^{-1})	$\alpha_i^{RO_2}$	k(NO_3) at 298K (molecules cm^{-3} s^{-1})	Average concentration at urban site (ppb) (mean±1σ)		Average concentration at rural site (ppb) (mean±1σ)	
					Daytime	Nighttime	Daytime	Nighttime
Alkanes								
1	Ethane	2.48E-13	0.019	1E-17	3.60±1.29	3.99±1.41	3.12±0.80	3.26±0.61
2	Propane	1.09E-12	0.036	7E-17	5.90±4.63	7.89±5.98	4.17±2.04	4.40±1.65
3	Iso-Butane	2.12E-12	0.096	/	1.73±1.39	2.04±1.50	1.61±0.87	1.71±0.71
4	n-Butane	2.36E-12	0.077	4.6E-17	3.05±2.56	3.62±2.74	3.10±1.83	3.32±1.49
5	Cyclopentane	4.97E-12	0.045	1.4E-16	0.09±0.05	0.09±0.06	0.13±0.09	0.15±0.08
6	Iso-Pentane	3.6E-12	0.07	/	1.22±1.05	1.47±1.27	1.78±1.90	2.88±3.06
7	n-Pentane	3.8E-11	0.105	8.7E-17	0.70±0.64	0.73±0.70	1.53±2.63	2.98±4.41
8	2,2-Dimethylbutane	2.23E-12	0.152	4.4E-16	0.04±0.03	0.04±0.03	0.03±0.02	0.03±0.02
9	2,3-Dimethylbutane	2.23E-12	0.152	4.4E-16	0.06±0.05	0.07±0.06	0.51±0.32	0.51±0.28
10	2 Methylpentane	5.2E-12	0.097	1.8E-16	0.35±0.33	0.41±0.39	/	/
11	3 Methylpentane	5.2E-12	0.109	2.2E-16	0.29±0.27	0.34±0.34	0.28±0.17	0.28±0.15
12	n-Hexane	5.2E-12	0.141	1.1E-16	0.68±0.89	0.65±0.85	0.37±0.25	0.41±0.26
13	Methylcyclopentane	5.6E-12	0.14	1.4E-16	0.10±0.10	0.12±0.12	0.10±0.07	0.10±0.06
14	Cyclohexane	6.97E-12	0.16	1.4E-16	0.08±0.08	0.08±0.08	0.08±0.11	0.09±0.17
15	2,4-Dimethylpentane	3.34E-12	0.14	/	0.04±0.03	0.03±0.03	0.04±0.03	0.05±0.08
16	2-Methylhexane	6.86E-12	0.205	1.5E-16	0.10±0.17	0.12±0.15	0.28±0.18	0.30±0.22
17	2,3-Dimethylpentane	/	/	1.5E-16	0.04±0.07	0.05±0.06	0.09±0.06	0.10±0.11
18	3-Methylhexane	7.15E-12	0.192	1.5E-16	0.12±0.21	0.15±0.20	0.29±0.20	0.29±0.22
19	n-Heptane	6.76E-12	0.178	1.5E-16	0.11±0.21	0.13±0.18	0.21±0.16	0.21±0.20
20	Methylcyclohexane	9.64E-12	0.17	1.4E-16	0.09±0.12	0.09±0.11	0.09±0.06	0.12±0.11
21	2,2,4-Trimethylpentane	3.34E-12	0.14	9E-17	0.03±0.02	0.04±0.03	0.06±0.07	0.08±0.14
22	2,3,4-Trimethylpentane	/	/	1.9E-16	0.01±0.01	0.02±0.01	0.06±0.08	0.07±0.15
23	2-Methylheptane	/	/	1.9E-16	0.02±0.03	0.02±0.03	0.10±0.14	0.12±0.19
24	3-Methylheptane	/	/	1.9E-16	0.02±0.03	0.02±0.03	0.11±0.15	0.13±0.20
25	n-Octane	8.11E-12	0.226	1.9E-16	0.04±0.05	0.05±0.04	0.21±0.15	0.25±0.18
26	Nonane	9.7E-12	0.393	2.3E-16	0.04±0.03	0.04±0.03	0.22±0.07	0.25±0.08
27	n-Decane	1.1E-11	0.417	2.8E-16	0.02±0.02	0.03±0.03	0.06±0.02	0.07±0.02
Alkenes								
28	Ethene	8.52E-12	0.0086	/	1.87±1.21	2.14±1.29	1.61±1.16	2.01±0.82
29	Propene	2.63E-11	0.015	9.54E-15	0.49±0.58	0.47±0.42	0.23±0.19	0.34±0.16
30	Trans-2-Butene	6.4E-11	0.034	/	0.04±0.03	0.05±0.05	0.001±0.007	0.001±0.01
31	1-Butene	3.14E-11	0.025	1.32E-14	0.08±0.06	0.09±0.07	0.03±0.04	0.06±0.04
32	Cis-2-Butene	5.64E-11	0.034	/	0.03±0.02	0.04±0.04	/	/
33	1-Pentene	3.14E-11	0.059	1.2E-14	0.03±0.01	0.03±0.02	0.003±0.007	0.006±0.01
34	Trans-2-Pentene	6.7E-11	0.064	/	0.01±0.02	0.02±0.04	0.002±0.006	0.005±0.01
35	Cis-2-Pentene	6.5E-11	0.064	3.7E-13	0.01±0.01	0.01±0.01	0.002±0.005	0.002±0.007
36	1-Hexene	3.7E-11	0.055	1.2E-14	0.02±0.01	0.02±0.01	0.004±0.008	0.01±0.01
37	Isoprene	1E-10	0.07	6.96E-13	0.18±0.15	0.06±0.06	0.24±0.21	0.03±0.04
38	Monoterpene	1.7E-10	0.23	1.22E-11	0.13±0.12	0.21±0.22	0.11±0.14	0.10±0.16
Aromatics								
39	Benzene	1.22E-12	0.034	3E-17	0.47±0.22	0.51±0.23	0.54±0.20	0.61±0.18
40	phenol	/	/	3.92E-12	0.04±0.02	0.04±0.03	0.06±0.03	0.04±0.02
41	Toluene	5.96E-12	0.029	7E-17	2.19±2.06	2.39±2.05	3.28±1.66	3.53±1.60
42	Ethylbenzene	7E-12	0.072	1.2E-16	0.32±0.31	0.39±0.35	0.86±0.47	1.13±0.72
43	m,p-Xylene	2.3E-11	0.074	3.8E-16	0.86±0.84	1.17±0.99	3.22±1.57	4.55±2.45
44	o-Xylene	1.36E-11	0.081	3.8E-16	0.32±0.33	0.43±0.38	1.10±0.61	1.57±0.98
45	Isopropylbenzene	6.3E-12	0.11	/	0.01±0.01	0.01±0.01	0.08±0.07	0.10±0.09
46	n-Propylbenzene	/	/	6E-16	0.01±0.01	0.02±0.01	0.10±0.04	0.10±0.06
47	m-Ethyltoluene	1.86E-11	0.094	/	0.03±0.03	0.04±0.04	0.13±0.04	0.15±0.06
48	p-Ethyltoluene	1.18E-11	0.137	/	0.02±0.02	0.03±0.02	0.14±0.05	0.16±0.07
49	1,3,5-Trimethylbenzene	5.76E-11	0.031	8.8E-16	0.02±0.02	0.02±0.02	0.12±0.03	0.14±0.04
50	o-Ethyltoluene	1.19E-11	0.106	/	0.02±0.01	0.02±0.02	0.10±0.02	0.11±0.03
51	1,2,4-Trimethylbenzene	3.25E-11	0.105	1.8E-15	0.06±0.07	0.09±0.09	0.09±0.05	0.11±0.06
52	1,2,3-Trimethylbenzene	3.25E-11	0.119	1.9E-15	0.02±0.01	0.02±0.02	0.05±0.02	0.06±0.02
Phenols								
53	cresol	/	/	1.37E-11	0.04±0.02	0.03±0.02	0.05±0.04	0.03±0.03
54	Styrene	5.8E-11	/	1.5E-12	0.11±0.19	0.17±0.24	0.28±0.29	0.57±0.75
Alkyne								
55	acetylene	/	/	5.1E-17	1.94±0.82	2.13±0.89	2.18±0.79	2.32±0.76

$\alpha_i^{RO_2}$ is yield of gaseous organonitrate in the reaction of RO_2 radical (from OH+VOC) with NO.

The ON yields (α_i^{NO3}) for isoprene (0.7), limonene (0.67), α-pinene (0.15), phenol (0.251), cresol (0.128) and styrene (0.251) were used in the calculation of NO_3-initiated pathway. The parameters of styrene were assumed equal to that of phenol.

The ON yields (α_i^{O3}) for isoprene (1.0), limonene (0.67), α-pinene (0.15) were used in the calculation of O_3-initiated pathway.

All OH and NO_3 reaction rate coefficients, ON formation yields $\alpha_i^{RO_2}$, α_i^{NO3}, and α_i^{O3} are from MCM v3.3.1 and previous study (Atkinson and Arey, 2003; Liebmann et al., 2019; Perring et al., 2013).

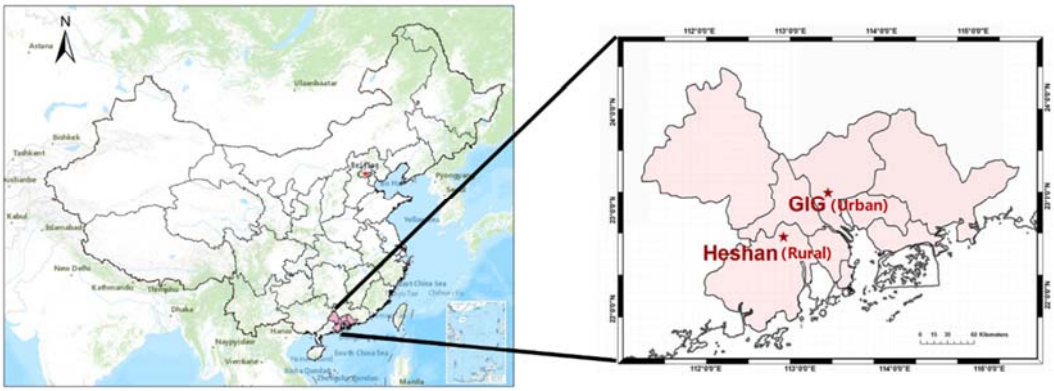

Figure S1. Location of the sampling sites.

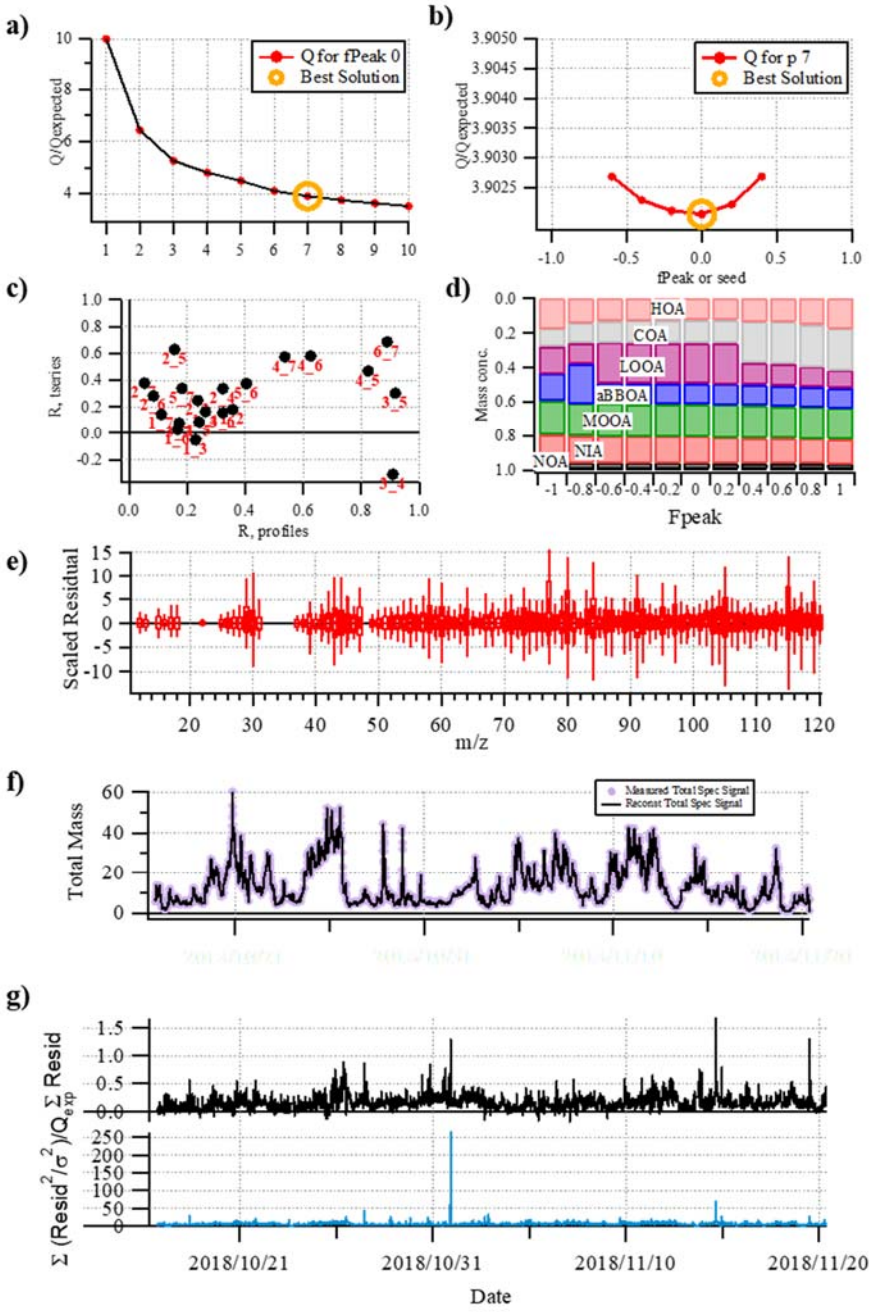

Figure S2. Diagnostic plots of the 7-factor solution in the $PMF_{Org+NOx}$ (laser off) at urban site.

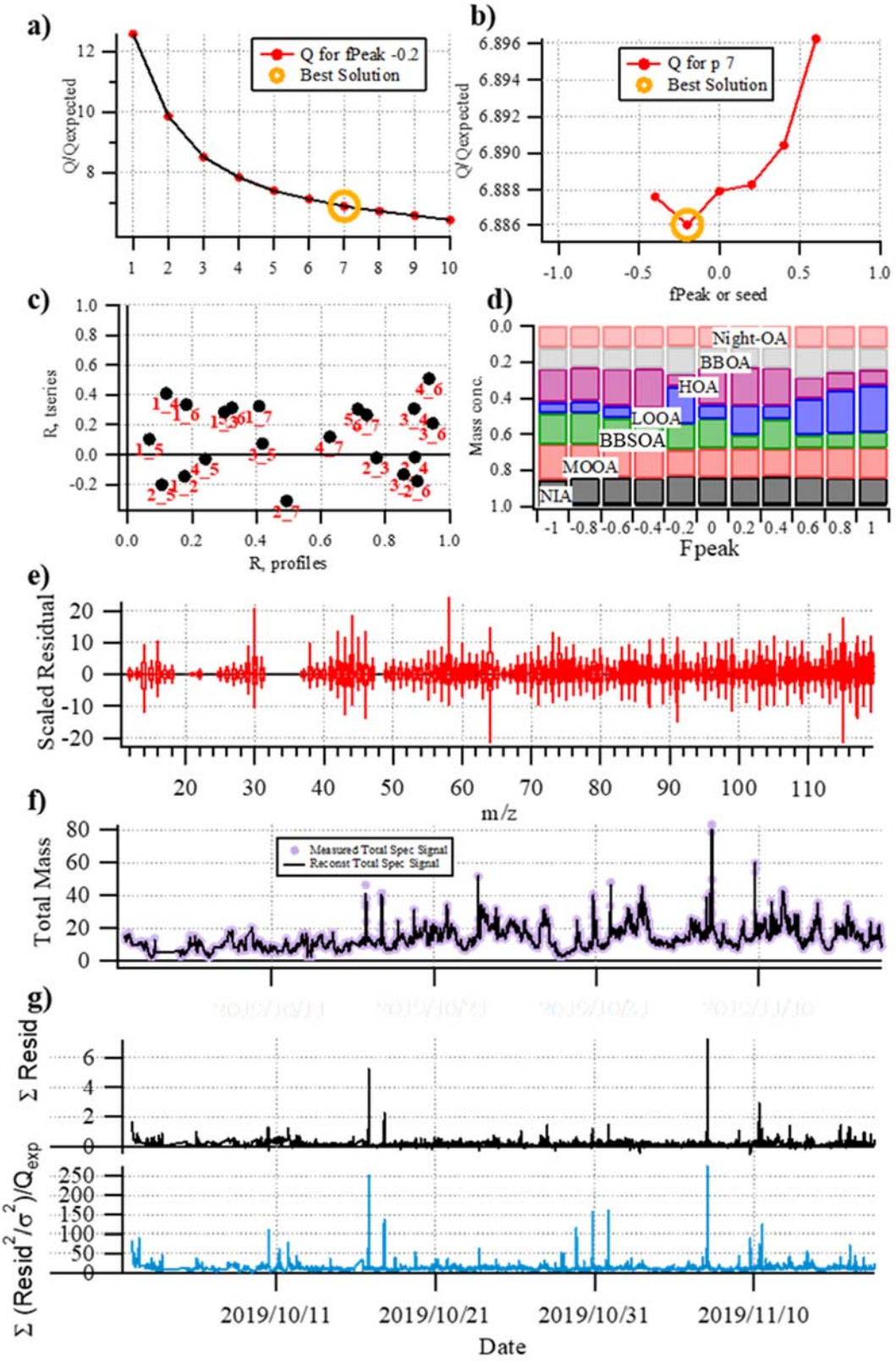

Figure S3. Diagnostic plots of the 7-factor solution in the $PMF_{Org+NOx}$ (laser off) at rural site.

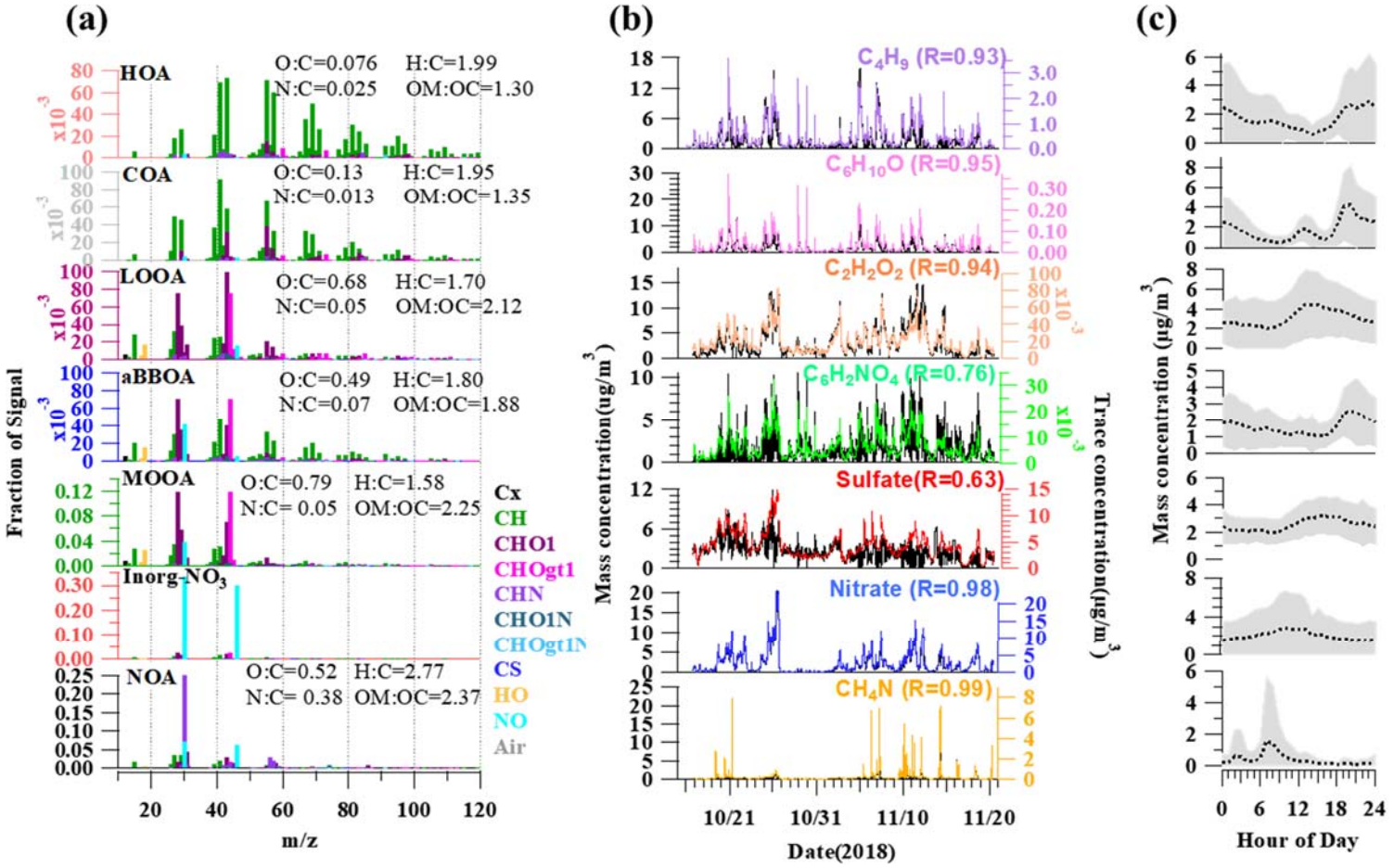

Figure S4. $PMF_{Org+NOx}$ (laser off) results at the urban site. **(a)** Mass spectra, **(b)** time series and **(c)** diurnal variations of seven factors based on high-resolution data.

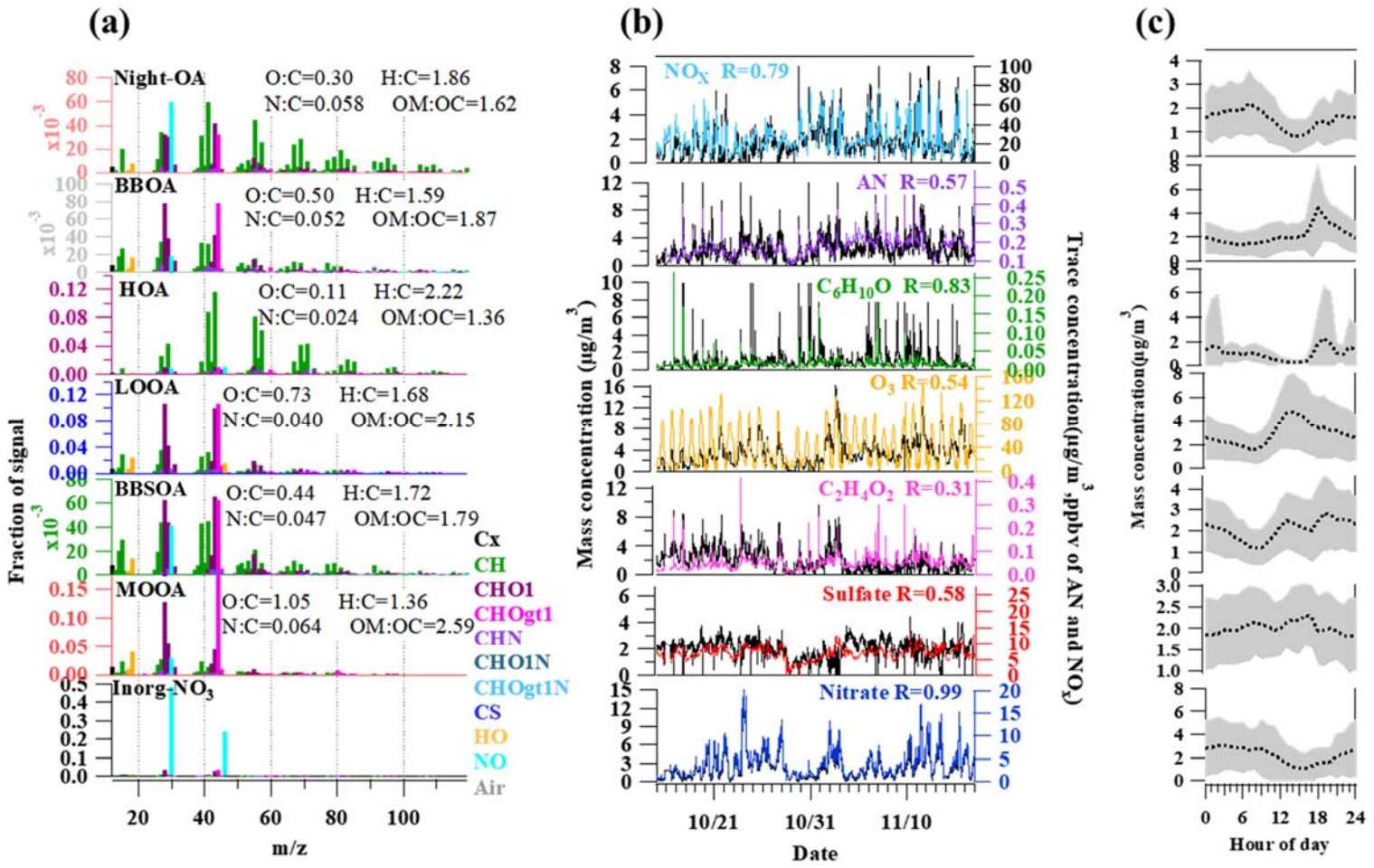

Figure S5. $PMF_{Org+NOx}$ (laser off) results at the rural site. **(a)** Mass spectra, **(b)** time series and **(c)** diurnal variations of seven factors based on high-resolution data.

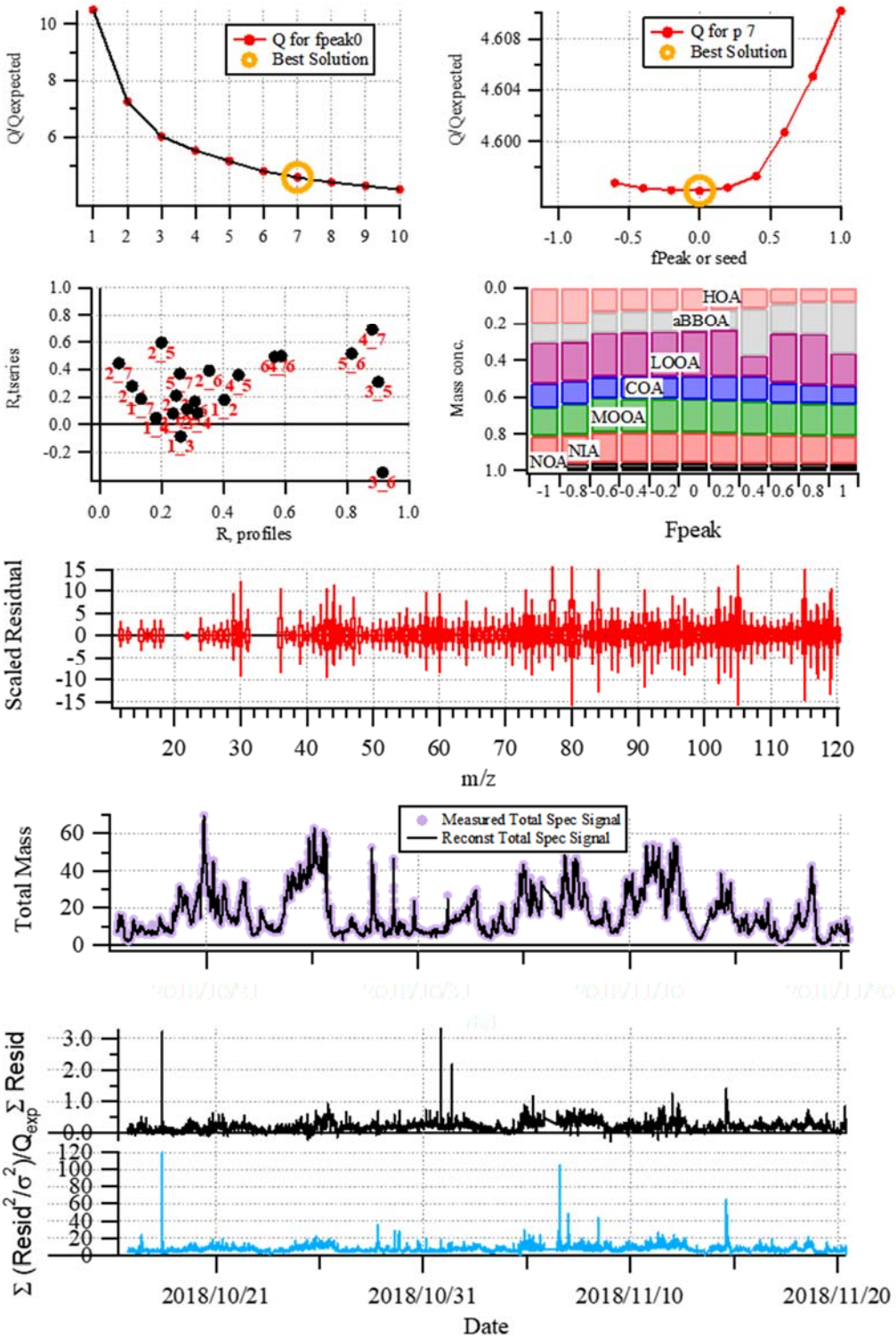

Figure S6. Diagnostic plots of the 7-factor solution in the $PMF_{Org+Cx+NOx}$ (laser on) at urban site.

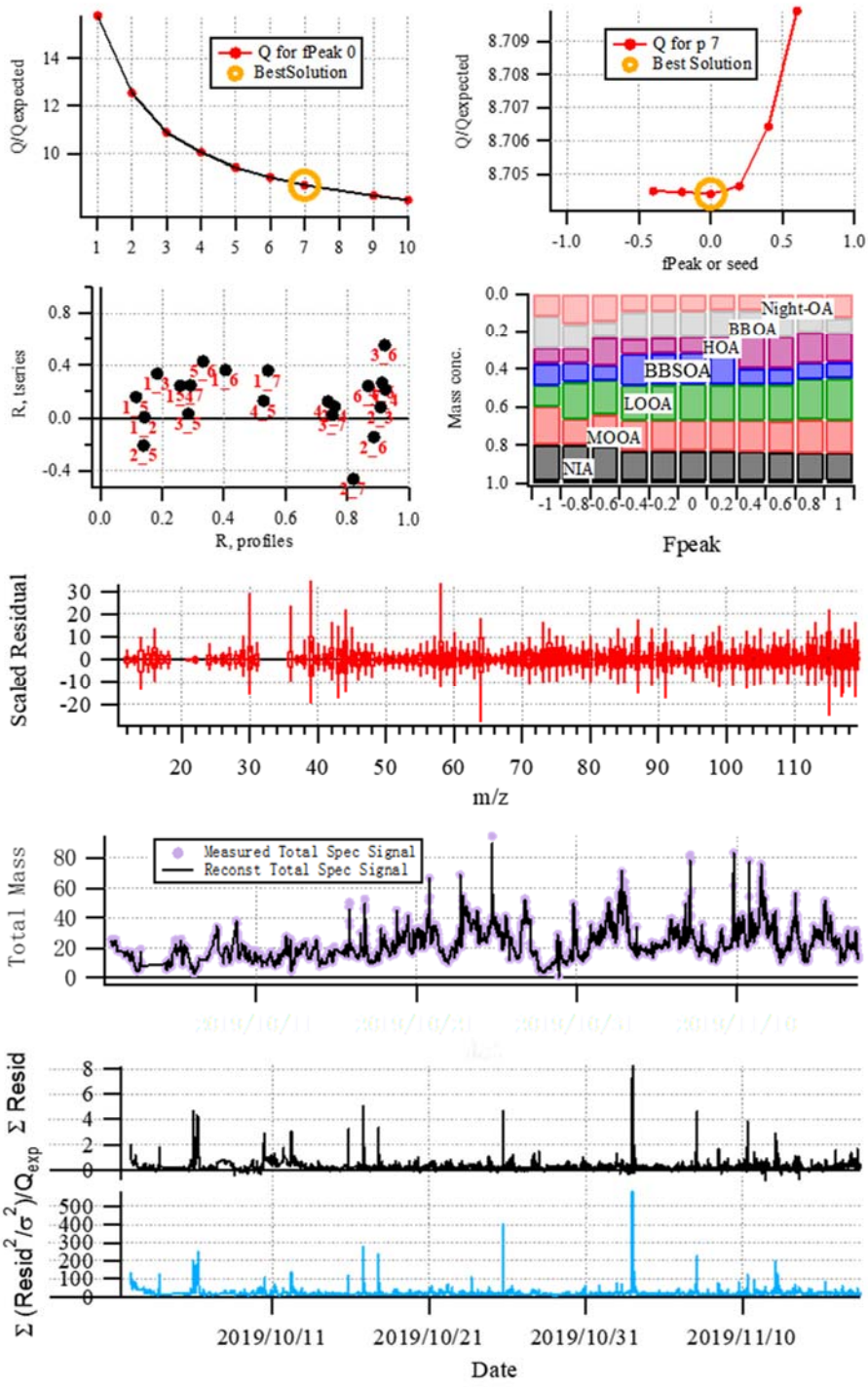

Figure S7. Diagnostic plots of the 7-factor solution in the $PMF_{Org+Cx+NOx}$ (laser on) at rural site.

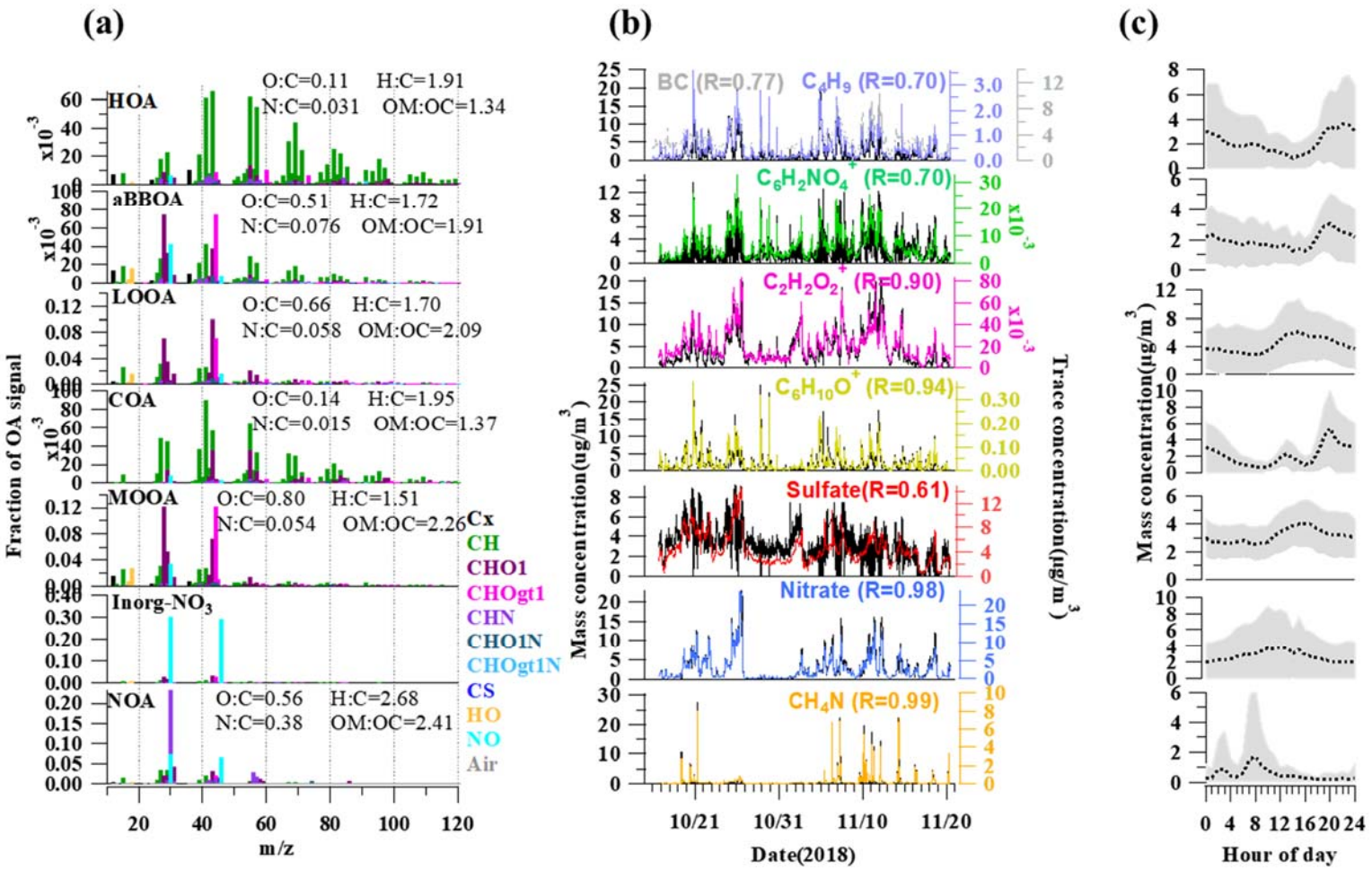

Figure S8. $PMF_{Org+Cx+NOx}$ (laser on) results at the urban site. **(a)** Mass spectra, **(b)** time series and **(c)** diurnal variations of seven factors based on high-resolution data.

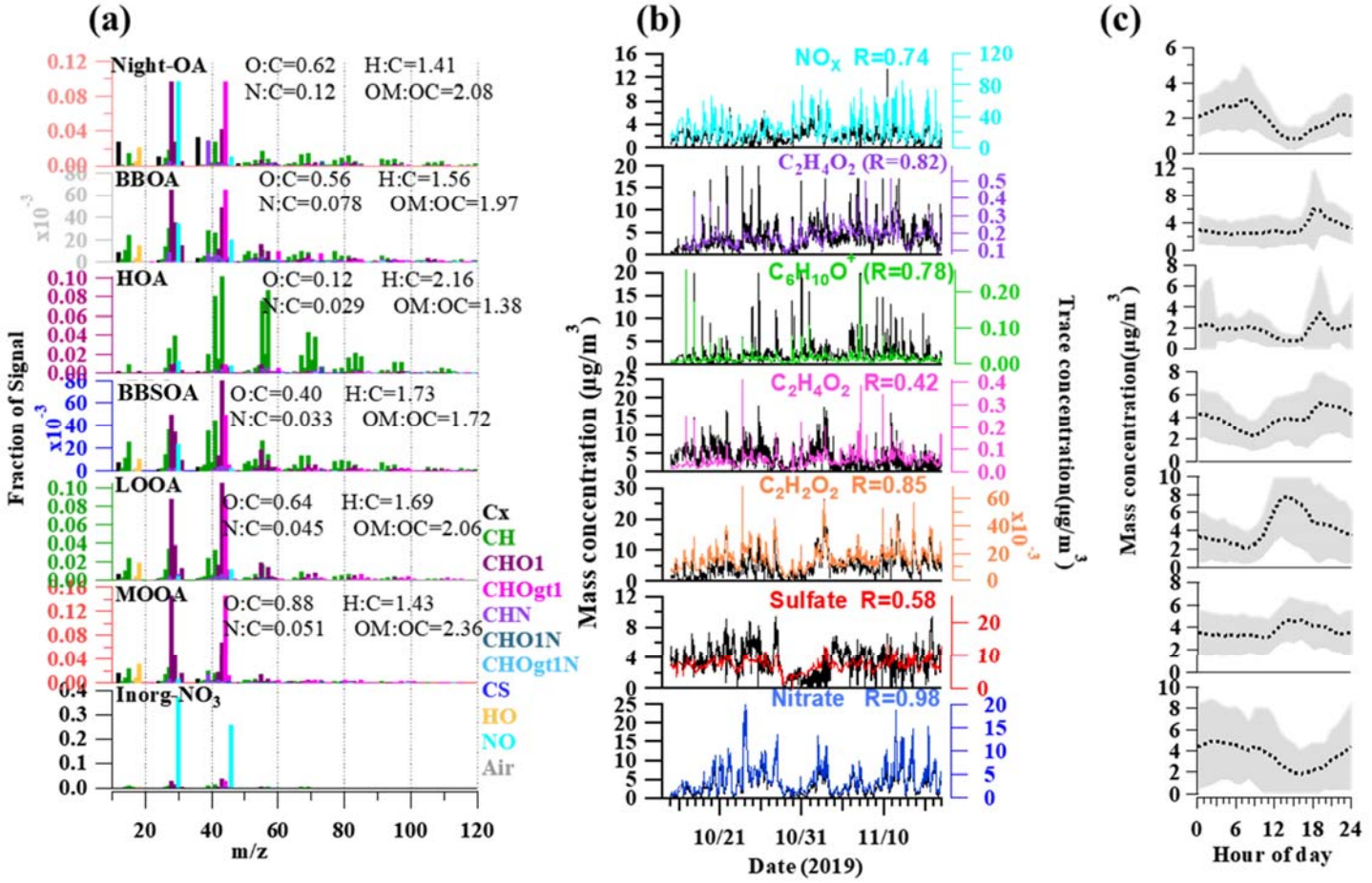

Figure S9. $PMF_{Org+Cx+NOx}$ (laser on) results at the rural site. **(a)** Mass spectra, **(b)** time series and **(c)** diurnal variations of seven factors based on high-resolution data.

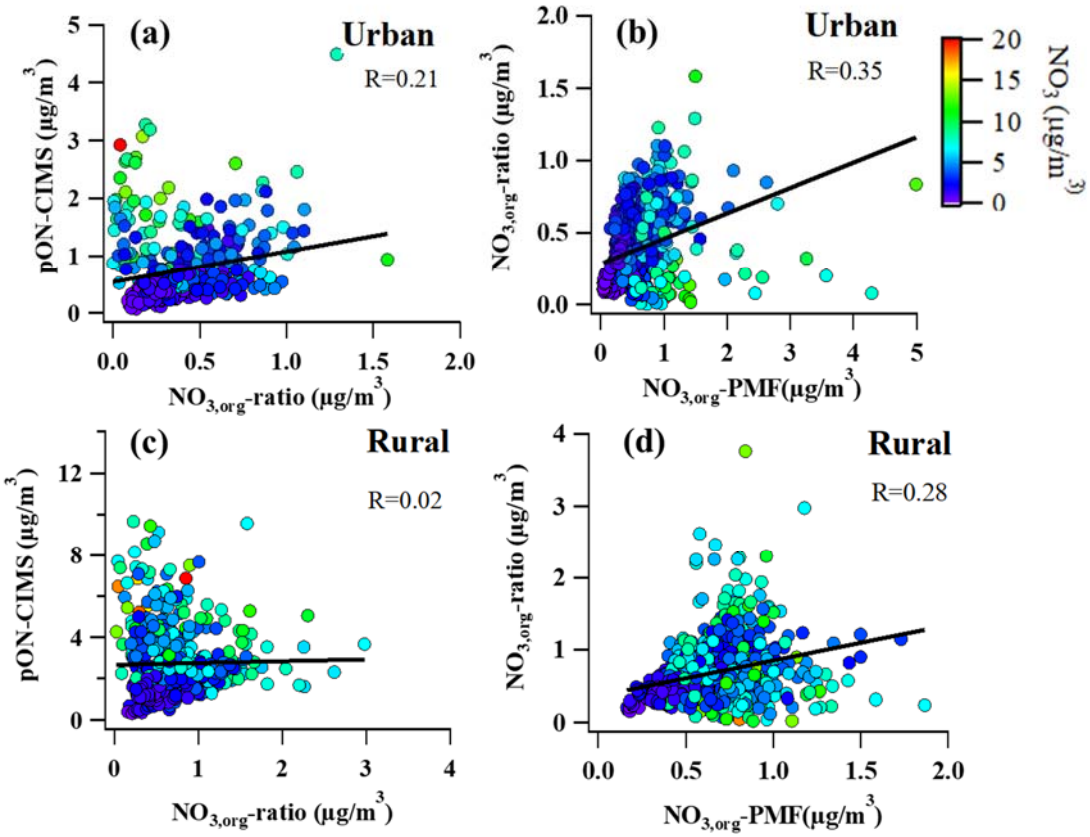

Figure S10. Comparison between pON from CIMS and $NO_{3,\,org}$ from the NO_x ratio method at (a) urban and (c) rural sites. Comparison between $NO_{3,\,org}$ from PMF method and NOx ratio method at (b) urban and (d) rural sites.

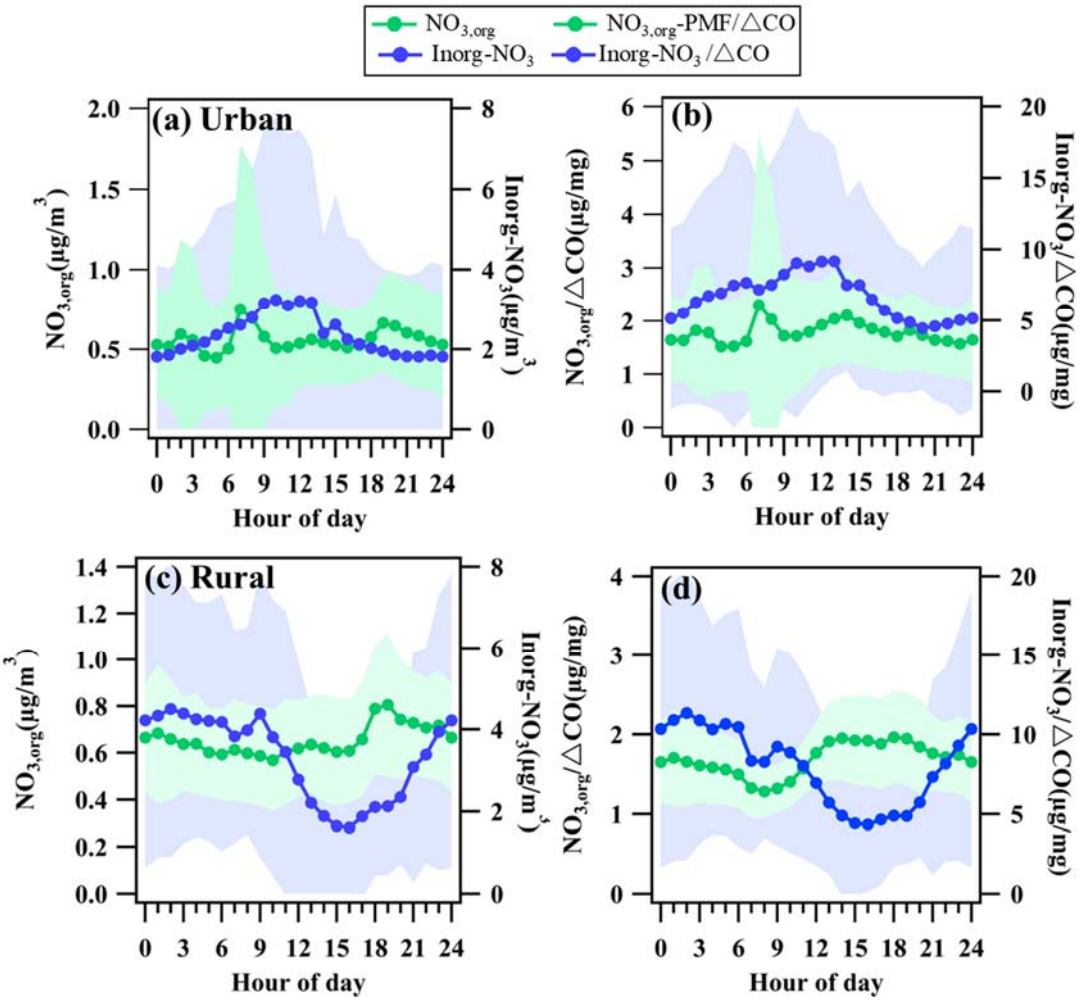

Figure S11. Diurnal variation of $NO_{3,org}$ and Inorg-NO_3 resolved by PMF methods at **(a)** urban and **(c)** rural site; Diurnal variations of $NO_{3,org}$ /ΔCO and Inorg-NO_3/ΔCO (ΔCO = CO-background CO) in **(b)** urban and **(d)** rural sites.

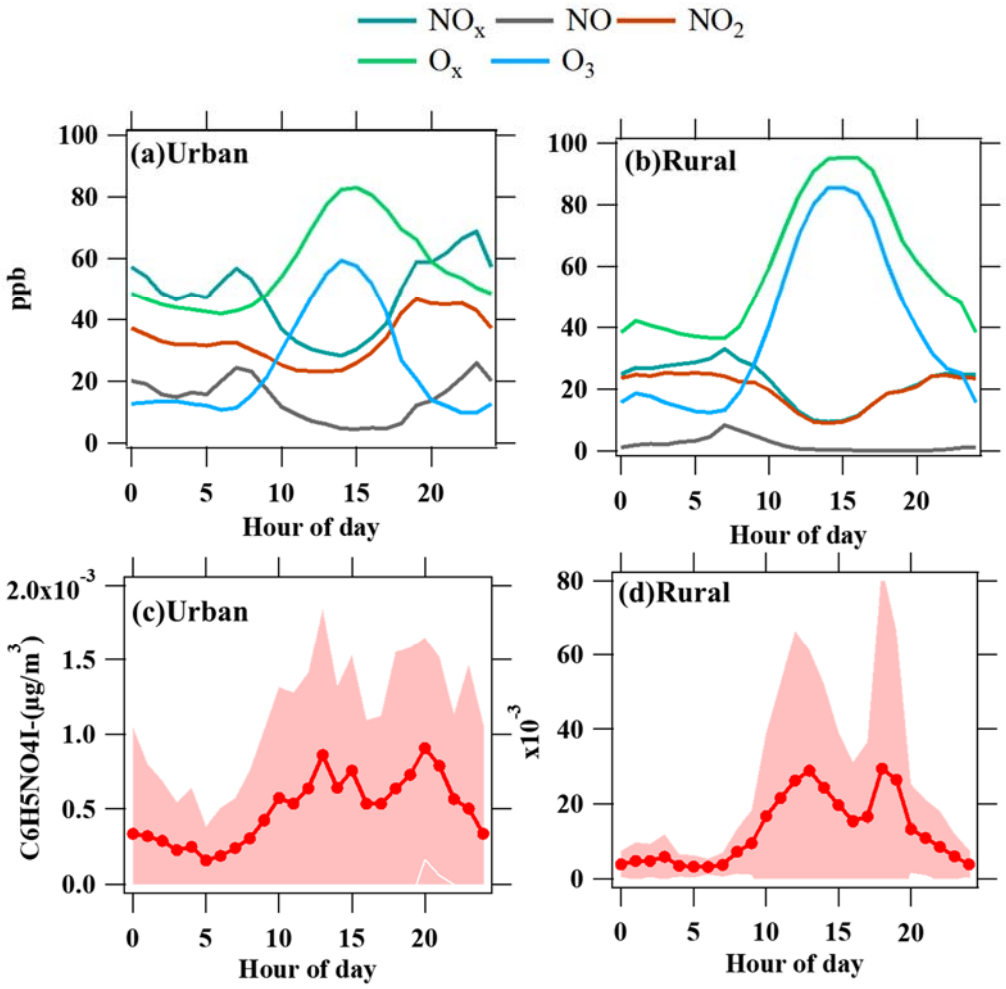

Figure S12. Diurnal variation of mixing ratios of nitrogen dioxide (NO_2), nitric oxide (NO), NO_x (NO_x = NO + NO_2), ozone (O_3) and O_x(O_3+NO_2) at the (a) urban and (b) rural sites. Diurnal variation of $C_6H_5NO_4I^-$ at (c)urban and (d) rural sites.

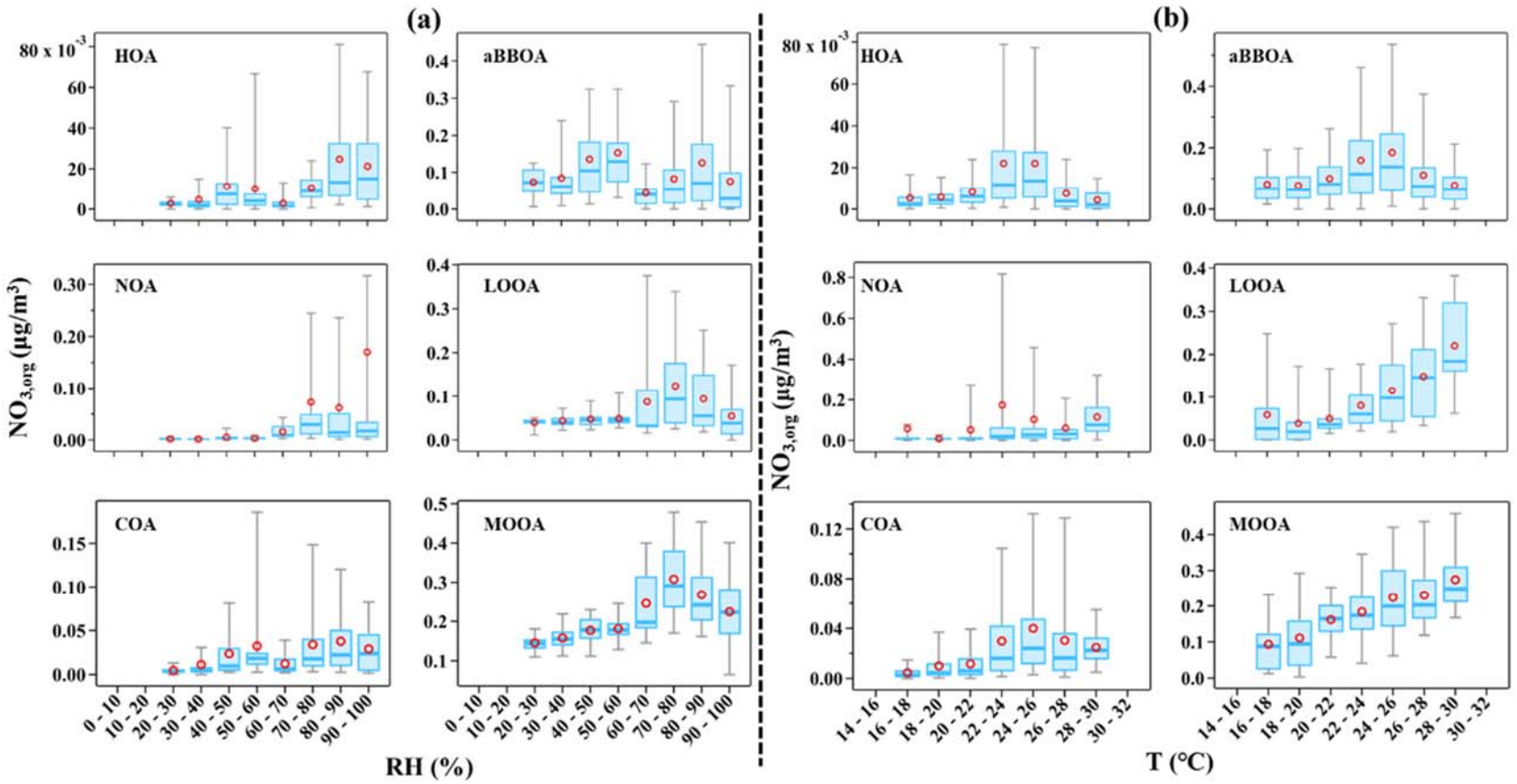

Figure S13. Variations of $NO_{3,org}$ associated with different OA factors as a function of (a)RH and (b)T at urban site. The mid-point line, lower and upper boxes, and lower and upper whiskers refer to the median, 25th and 75th percentiles, and 10th and 90th percentiles, respectively, for the study period. Red circles represent averages.

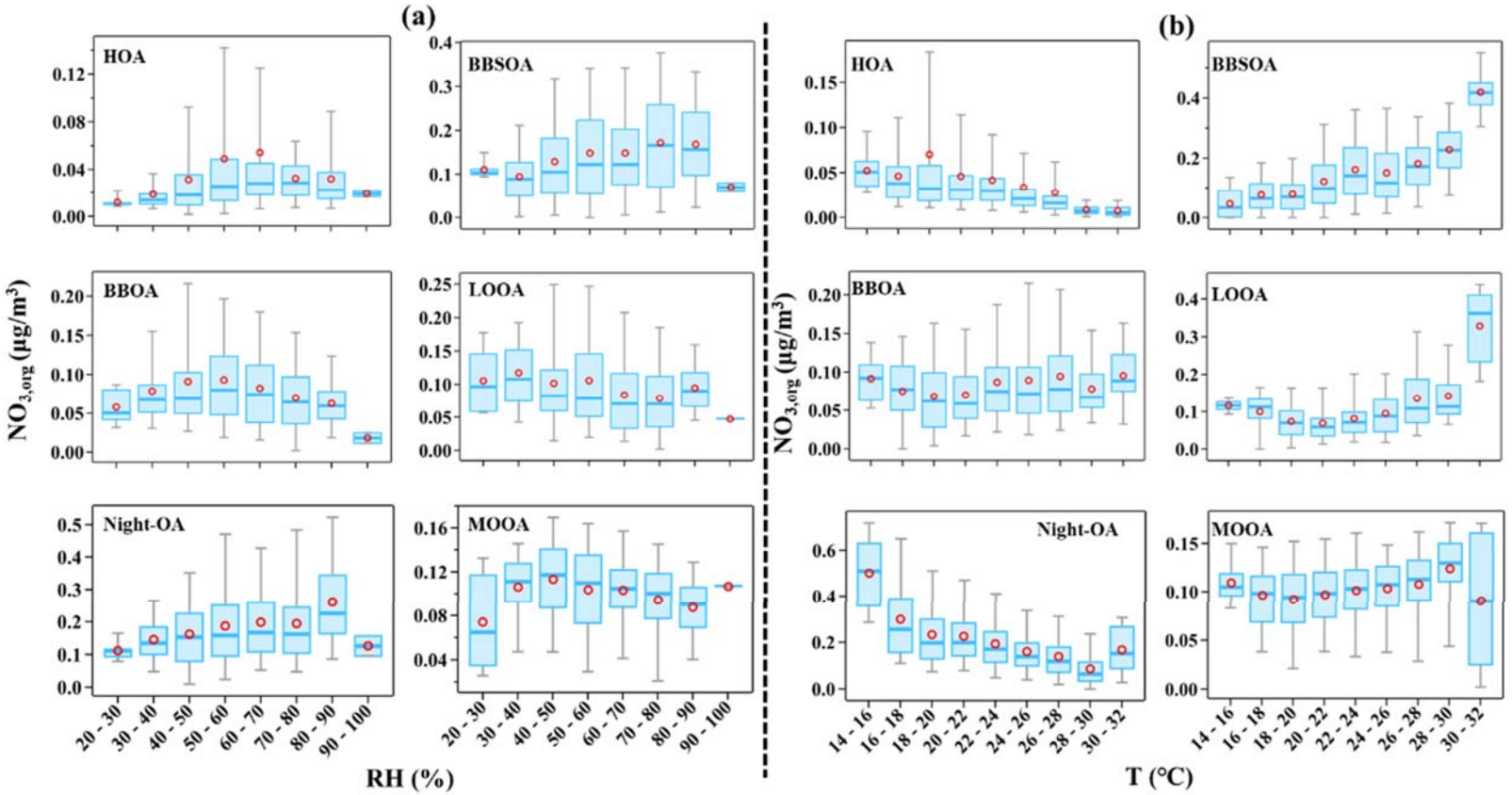

Figure S14. Variations of $NO_{3,org}$ associated with different OA factors as a function of (a)RH and (b)T at rural site. The mid-point line, lower and upper boxes, and lower and upper whiskers refer to the median, 25th and 75th percentiles, and 10th and 90th percentiles, respectively, for the study period. Red circles represent averages.

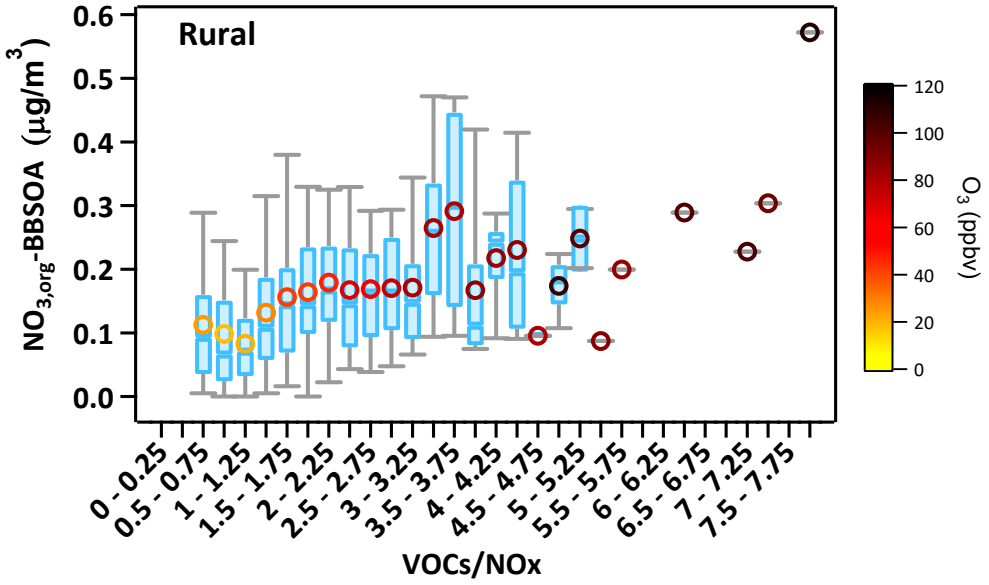

Figure S15 $NO_{3,org}$-BBSOA as a function of VOCs/NOx ratio at rural site colored by O3 concentration.

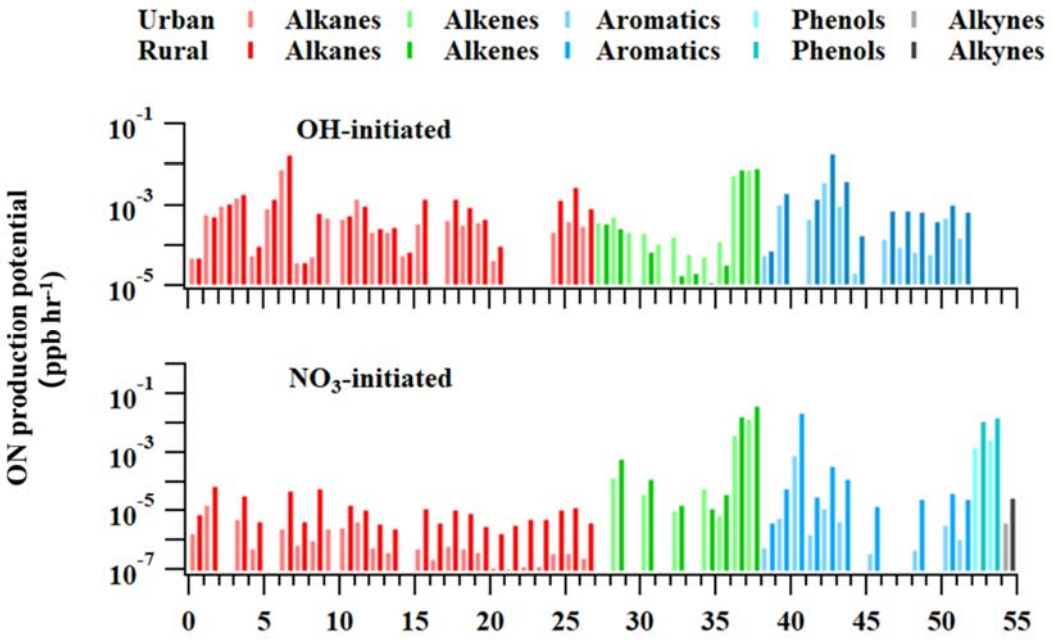

Figure S16 Calculated PP_{ON} of (a) OH-initiated and (b) of NO_3-initiated during the campaign at urban (half-transparent sticks) and rural site (solid sticks). The number of horizontal axes represents corresponding VOCs in Table S4.

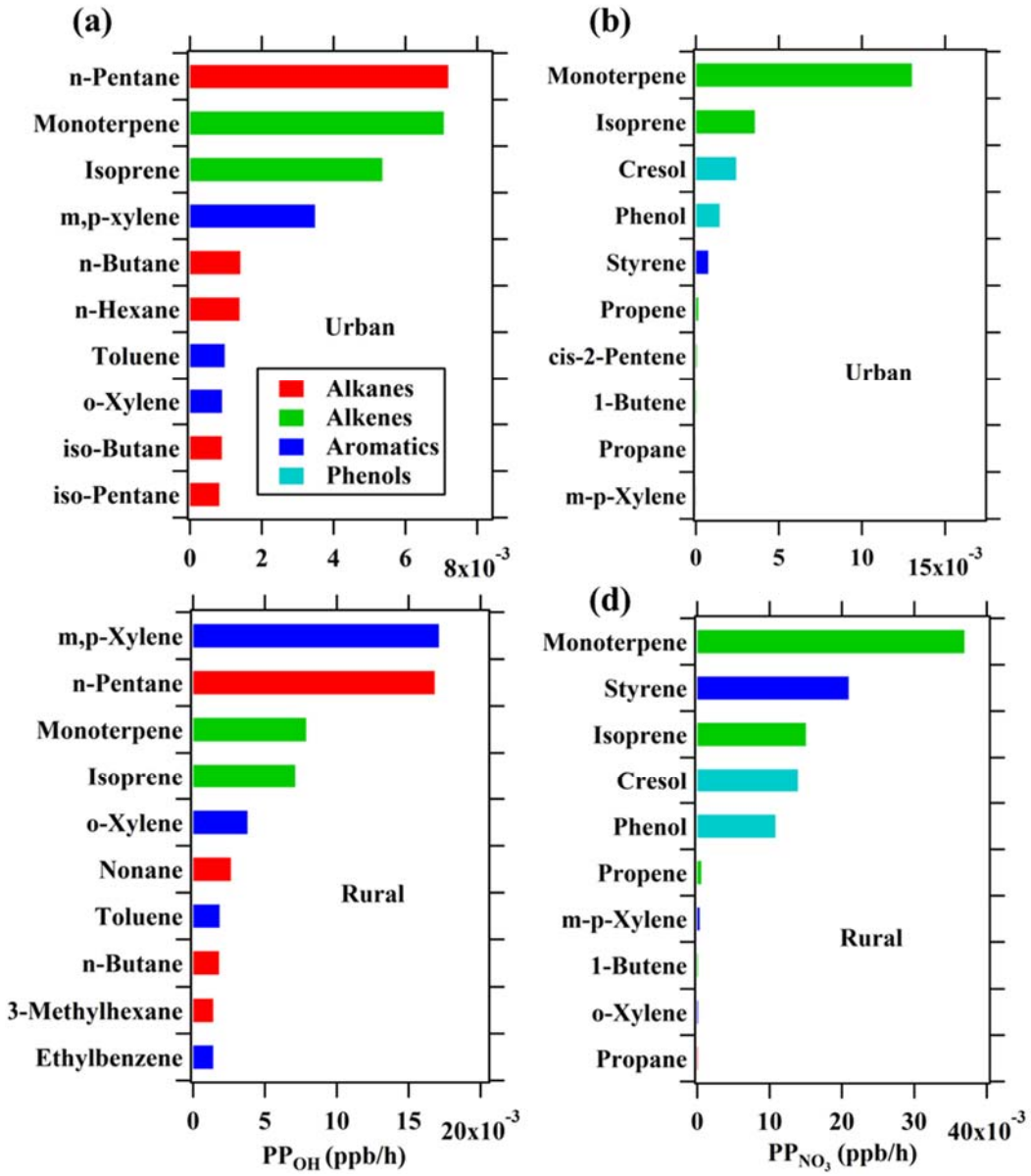

Figure S17. Top ten VOCs with PP_{OH} and PP_{NO3} at **(a)(c)** urban and **(b)(d)** rural site.

Reference

Atkinson R., and Arey, J.: Atmospheric degradation of volatile organic compounds, Chemical reviews, 2003, 103(12), 4605-4638.

Boyd C. M., Sanchez, J., Xu, L., Eugene, A. J., Nah, T., Tuet, W. Y., Guzman, M. I., and Ng, N. L.: Secondary organic aerosol formation from the β-pinene+NO3 system: effect of humidity and peroxy radical fate, Atmospheric Chemistry and Physics, 2015, 15(13), 7497-7522, doi:10.5194/acp-15-7497-2015.

Bruns E. A., Perraud, V., Zelenyuk, A., Ezell, M. J., Johnson, S. N., Yu, Y., Imre, D., Finlayson-Pitts, B. J., and Alexander, M. L.: Comparison of FTIR and particle mass spectrometry for the measurement of particulate organic nitrates, Environmental science & technology, 2010, 44(3), 1056-1061.

Day D. A., Campuzano-Jost, P., Nault, B. A., Palm, B. B., Hu, W., Guo, H., Wooldridge, P. J., Cohen, R. C., Docherty, K. S., Huffman, J. A., de Sá, S. S., Martin, S. T., and Jimenez, J. L.: A systematic re-evaluation of methods for quantification of bulk particle-phase organic nitrates using real-time aerosol mass spectrometry, Atmos. Meas. Tech., 2022, 15(2), 459-483, doi:10.5194/amt-15-459-2022.

Farmer D. K., Matsunaga, A., Docherty, K. S., Surratt, J. D., Seinfeld, J. H., Ziemann, P. J., and Jimenez, J. L.: Response of an aerosol mass spectrometer to organonitrates and organosulfates and implications for atmospheric chemistry, Proc Natl Acad Sci U S A, 2010, 107(15), 6670-6675, doi:10.1073/pnas.0912340107.

Fry J., Kiendler-Scharr, A., Rollins, A., Wooldridge, P., Brown, S., Fuchs, H., Dubé, W., Mensah, A., Dal Maso, M., and Tillmann, R.: Organic nitrate and secondary organic aerosol yield from NO 3 oxidation of β-pinene evaluated using a gas-phase kinetics/aerosol partitioning model, Atmospheric Chemistry and Physics, 2009, 9(4), 1431-1449.

Liao Y., Yu, M., Liang, L., Wang, X., Yin, J., Fang, Z., Chang, M., Yuan, B., Shao, M., and Huang, S.: Sources and characteristic components of atmospheric organic aerosols in the autumn suburbs of Guangzhou, China Environmental Sciences, 2026, 46(1), 53-65.

Liebmann J., Sobanski, N., Schuladen, J., Karu, E., Hellén, H., Hakola, H., Zha, Q., Ehn, M., Riva, M., Heikkinen, L., Williams, J., Fischer, H., Lelieveld, J., and Crowley, J. N.: Alkyl nitrates in the boreal forest: formation via the NO3-, OH- and O3-induced oxidation of biogenic volatile organic compounds and ambient lifetimes, Atmospheric Chemistry and Physics, 2019, 19(15), 10391-10403, doi:10.5194/acp-19-10391-2019.

Perring A. E., Pusede, S. E., and Cohen, R. C.: An observational perspective on the atmospheric impacts of alkyl and multifunctional nitrates on ozone and secondary organic aerosol, Chem Rev, 2013, 113(8), 5848-5870, doi:10.1021/cr300520x.